[2] M. J. Berger and J. R. Oliger, "Adaptive mesh refinement for hyperbolic partial differential equation," *J. Comput. Phys.*, vol. 53, pp. 484–512, 1984.
[3] R. Holland and L. Simpson, "Finite difference analysis of EMP coupling to thin struts and wires," *IEEE Trans. Electromagn. Compat.*, vol. EMC-23, pp. 88–97, May 1981.
[4] K. S. Kunz and L. Simpson, "A technique for increasing the resolution of finite-difference solution of the Maxwell equation," *IEEE Trans. Electromagn. Compat.* vol. EMC-23, pp. 419–422, Nov. 1981.
[5] G. Browning, H-O. Kreiss, and J. R. Oliger, "Mesh refinement," *Math. Comput.*, vol. 27, no. 121, pp. 29–39, Jan. 1973.

Frequency-Domain Bivariate Generalized Power Series Analysis of Nonlinear Analog Circuits

PHILIP J. LUNSFORD II, STUDENT MEMBER, IEEE,
GEORGE W. RHYNE, MEMBER, IEEE, AND
MICHAEL B. STEER, MEMBER, IEEE

Abstract—**Bivariate generalized power series analysis is introduced for the analysis and behavioral modeling of nonlinear analog circuits and systems. It can be used to model analog subsystems and is compatible with circuit simulation. Thus full circuits and behaviorally modeled analog subcircuits can be simulated together in an analog circuit/system simulator. The entire analysis is performed in the frequency domain, and arbitrary nonlinear circuits and any number of noncommensurable input frequencies can be handled. A diode ring demodulator is analyzed as an example.**

I. Introduction

The simulation of complex analog circuits using harmonic balance and spectral balance techniques has developed rapidly in recent years. The analysis of nonlinear analog systems using behavioral modeling of nonlinear subsystems is less advanced, with Volterra series system analysis being the dominant method [1]. This technique, however, is limited to mildly nonlinear systems.

In this paper we present a frequency-domain modeling method that is an extension of the generalized power series analysis (GPSA), introduced by Steer and Khan [2]. GPSA is a frequency-domain simulation technique based on power series that, in general, can contain complex coefficients. However, GPSA can only be used with elements or systems having a single voltage or current controlling excitation. The bivariate GPSA introduced here can be used with elements or subsystems that have two controlling quantities and is more general than the power series method proposed by Narhi [3].

As an example, we present a behavioral model for a diode ring mixer. This mixer, shown in Fig. 1, can be analyzed using a univariate power series to describe the current–voltage characteristics of each diode, but this method requires the use of iterative techniques to satisfy Kirchhoff's voltage and current laws for the circuit [4]. The behavioral model presented here can be used as a voltage-controlled voltage source in a GPSA simulator such as FREDA [4] or in a block system simulator such as CAPSIM [5].

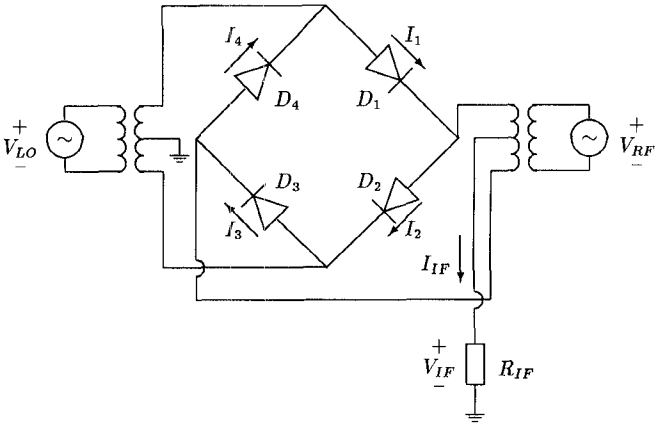

Fig. 1. Diode ring mixer.

II. Development of Algebraic Formulas

In this section we derive an algebraic formula for the output components of a nonlinearity which can be described by a power series in two variables having complex coefficients and frequency-dependent time delays when the inputs are sums of sinusoids.

A nonlinear element or system having the two multifrequency inputs $x(t)$ and $z(t)$ (each having N components),

$$x(t) = \sum_{k=1}^{N} x_k(t) = \sum_{k=1}^{N} |X_k| \cos(\omega_k t + \phi_k) \tag{1}$$

and

$$z(t) = \sum_{k=1}^{N} z_k(t) = \sum_{k=1}^{N} |Z_k| \cos(\omega_k t + \theta_k) \tag{2}$$

can be represented by the bivariate generalized power series

$$y(t) = \sum_{\sigma=0}^{\infty} \sum_{\rho=0}^{\infty} a_{\sigma,\rho} f(\sigma, x) g(\rho, z) \tag{3}$$

with

$$f(\sigma, x) = \left(\sum_{k=1}^{N} b_k x_k(t - \tau_{k,\sigma}) \right)^{\sigma} \tag{4}$$

and

$$g(\rho, z) = \left(\sum_{k=1}^{N} d_k z_k(t - \lambda_{k,\rho}) \right)^{\rho}. \tag{5}$$

In these expressions, $a_{\sigma,\rho}$ is a complex coefficient, b_k and d_k are real, and $\tau_{k,\sigma}$ and $\lambda_{k,\rho}$ are time delays that depend on both the order of the power series and the index of the input frequency components. Our aim is to rewrite (3) in terms of phasors. The x input can be expressed as

$$\begin{aligned} x_k(t - \tau_{k,\sigma}) &= |X_k| \cos(\omega_k t + \phi_k - \omega_k \tau_{k,\sigma}) \\ &= \frac{1}{2} X_k \Gamma_{k,\sigma} e^{j\omega_k t} + \frac{1}{2} X_k^* \Gamma_{k,\sigma}^* e^{-j\omega_k t} \end{aligned} \tag{6}$$

Manuscript received October 2, 1989; revised January 17, 1990. This work was supported by an NSF Presidential Young Investigator Award (ECS-8657836) to M. B. Steer and by IBM.

P. J. Lunsford II is with IBM, mailstop D63/061, P.O. Box 12195, Research Triangle Park, NC 27709.
G. W. Rhyne was with the Department of Electrical and Computer Engineering, North Carolina State University, Raleigh, NC 27695. He is now with Motorola Corporate Research Laboratories, 2100 East Elliot Rd., Tempe, AZ 85284.
M. B. Steer is with the Department of Electrical and Computer Engineering, North Carolina State University, Raleigh, NC 27695-7911.

IEEE Log Number 9034848.

where X_k is the phasor of $x_k(t)$ and

$$\Gamma_{k,\sigma} = e^{-j\omega_k \tau_{k,\sigma}}. \tag{7}$$

Similarly, for the other input $z(t)$, we write

$$\begin{aligned} z_k(t-\lambda_{k,\rho}) &= |Z_k|\cos(\omega_k t + \theta_k - \omega_k \lambda_{k,\rho}) \\ &= \frac{1}{2} Z_k \Upsilon_{k,\rho} e^{j\omega_k t} + \frac{1}{2} Z_k^* \Upsilon_{k,\rho}^* e^{-j\omega_k t} \end{aligned} \tag{8}$$

where Z_k is the phasor of $z_k(t)$ and

$$\Upsilon_{k,\rho} = e^{-j\omega_k \lambda_{k,\rho}}. \tag{9}$$

Using the multinomial expansion theorem [6], we write (4) as

$$\begin{aligned} f(\sigma,x) = & \underbrace{\sum}_{\substack{l_1,\cdots,l_N,m_1,\cdots,m_N \\ l_1+\cdots+l_N+m_1+\cdots+m_N=\sigma}} \left\{ \left[\exp\left(j \sum_{k=1}^{N} (l_k - m_k)\omega_k t \right) \right] \sigma! \right. \\ & \left. \cdot \prod_{k=1}^{N} \left(\frac{\left(\frac{1}{2} b_k\right)^{l_k+m_k} (X_k)^{l_k} (X_k^*)^{m_k} (\Gamma_{k,\sigma})^{l_k} (\Gamma_{k,\sigma}^*)^{m_k}}{l_k! m_k!} \right) \right\} \end{aligned} \tag{10}$$

where the summation is over all combinations of the integers $l_1,\cdots,l_N,m_1,\cdots,m_n$ such that $\sum_{k=1}^{N} l_k + m_k = \sigma$. Similarly, we can expand (5), and the product of f and g becomes

$$\begin{aligned} f(\sigma,x)g(\rho,z) = & \underbrace{\sum}_{\substack{l_1,\cdots,l_N,m_1,\cdots,m_N \\ i_1,\cdots,i_N,j_1,\cdots,j_N \\ l_1+\cdots+l_N+m_1+\cdots+m_N=\sigma \\ i_1+\cdots+i_N+j_1+\cdots+j_N=\rho}} \left[\exp\left(j \sum_{k=1}^{N} (l_k + i_k - m_k - j_k)\omega_k t \right) \right] \sigma!\rho!\Psi \end{aligned}$$

where

$$\Psi = \prod_{k=1}^{N} \frac{\left(\frac{1}{2} b_k\right)^{l_k+m_k} \left(\frac{1}{2} d_k\right)^{i_k+j_k} (X_k)^{l_k} (X_k^*)^{m_k} (Z_k)^{i_k} (Z_k^*)^{j_k} (\Gamma_{k,\sigma})^{l_k} (\Gamma_{k,\sigma}^*)^{m_k} (\Upsilon_{k,\rho})^{i_k} (\Upsilon_{k,\rho}^*)^{j_k}}{l_k! m_k! i_k! j_k!}$$

and the above summation is over all combinations of the nonnegative integers l, m, i, and j such that $\sum_{k=1}^{N} l_k + m_k = \sigma$ and $\sum_{k=1}^{N} i_k + j_k = \rho$. As with the single-variable power series, the frequency of each component is

$$\omega = \sum_{k=1}^{N} n_k \omega_k \tag{11}$$

where n_k is a set of integers, an intermodulation product description (IPD) where $n_k = l_k + i_k - m_k - j_k$. The intermodulation order is n, where $n = \sum_{k=1}^{N} |n_k|$. Letting $(p_k + q_k)$ equal the larger of $(l_k + i_k)$ and $(m_k + j_k)$, and $(r_k + s_k)$ equal the smaller, we have $p_k + q_k - r_k - s_k = |n_k|$ where p_k, q_k, r_k, and $s_k \geq 0$.

For a given set of n_k's specifying an individual intermodulation product (IP), the relevant components of $f(\sigma,x)g(\rho,z)$ can be written as the sum of two terms (for $n \neq 0$):

$$\begin{aligned} & \left(\frac{1}{2}C\right) e^{j\omega_q t} + \left(\frac{1}{2}C\right)^* e^{-j\omega_q t} \\ & = \left(\frac{1}{2}U_q'\right) e^{j\omega_q t} + \left(\frac{1}{2}U_q'\right)^* e^{-j\omega_q t}, \qquad \omega_q \neq 0 \\ & = U_q', \qquad \omega_q = 0 \end{aligned} \tag{12}$$

where

$$C = 2 \underbrace{\sum}_{\substack{p_1,\cdots,p_N,r_1,\cdots,r_N \\ q_1,\cdots,q_N,s_1,\cdots,s_N \\ p_1+\cdots+p_N+r_1+\cdots+r_N=\sigma \\ q_1+\cdots+q_N+s_1+\cdots+s_N=\rho \\ p_k+q_k-r_k-s_k=|n_k|}} \left\{ \left(\frac{1}{2}\right)^{\sigma+\rho} \sigma!\rho!\Phi \right\} \tag{13}$$

and with

$$\Phi = \prod_{k=1}^{N} \frac{(b_k)^{p_k+r_k} (d_k)^{q_k+s_k} (X_k^\dagger)^{p_k} (X_k^\ddagger)^{r_k} (Z_k^\dagger)^{q_k} (Z_k^\ddagger)^{s_k} (\Gamma_{k,\sigma}^\dagger)^{p_k} (\Gamma_{k,\sigma}^\ddagger)^{r_k} (\Upsilon_{k,\rho}^\dagger)^{q_k} (\Upsilon_{k,\rho}^\ddagger)^{s_k}}{p_k! r_k! q_k! s_k!}. \tag{14}$$

Here we define

$$X_k^\dagger = \begin{cases} X_k & \text{for } n_k \geq 0 \\ X_k^* & \text{for } n_k < 0 \end{cases}$$

and

$$X_k^\ddagger = \begin{cases} X_k^* & \text{for } n_k \geq 0 \\ X_k & \text{for } n_k < 0. \end{cases}$$

($Z_k^\dagger$, $Z_k^\ddagger$, $\Gamma_{k,\sigma}^\dagger$, $\Gamma_{k,\sigma}^\ddagger$, $\Upsilon_{k,\rho}^\dagger$, and $\Upsilon_{k,\rho}^\ddagger$ are similarly defined.) Thus,

$$U_q' = \begin{cases} C & \text{for } \omega_q \neq 0 \\ \frac{1}{2}(C + C^*) = \mathrm{Re}(C) & \text{for } n \neq 0 \text{ and } \omega_q = 0. \end{cases} \tag{15}$$

Note that U_q' is the contribution to $f(\sigma,x)g(\rho,y)$ of one IP. When the two terms in (12) occur for $n \neq 0$, p_k and q_k replace two sets of i_k, j_k, l_k, and m_k, one set corresponding to $(l_k + i_k) > (m_k + j_k)$, resulting in the $e^{j\omega_q t}$ term and the other corresponding to $(l_k + i_k) < (m_k + j_k)$, resulting in the $e^{-j\omega_q t}$ term. For $n = 0$ there is only one set corresponding to $(l_k + i_k) = (m_k + j_k)$. Thus, the U_q' expression is half that in (15) for the case $n = 0$. For (15) to hold we make the restriction that no IPD be equal to the negative of another IPD. If U_q is the component of Y due to a single intermodulation product, then

$$U_q = \sum_{\sigma=0}^{\infty} \sum_{\rho=0}^{\infty} a_{\sigma,\rho} U_q'. \tag{16}$$

Using the Neumann factor, $\epsilon_n(\epsilon_n = 1,\ n = 0;\ \epsilon_n = 2,\ n \neq 0)$,

$$U_q = \mathrm{Re}\{\epsilon_n T\}_{\omega_q} \tag{17}$$

where $\mathrm{Re}\{\ \}_{\omega_q}$ is defined such that it is ignored for $\omega_q \neq 0$ but for $\omega_q = 0$ the real part of the expression in brackets is taken. In (17)

$$T = \sum_{\alpha=0}^{\infty} \sum_{\substack{p_1,\cdots,p_N,r_1,\cdots,r_N \\ \underbrace{q_1,\cdots,q_N,s_1,\cdots,s_N}} \\ \substack{p_1+\cdots+p_N+r_1+\cdots+r_N=\sigma \\ q_1+\cdots+q_N+s_1+\cdots+s_N=\rho \\ p_k+q_k-r_k-s_k=|n_k| \\ \sigma+\rho=n+2\alpha}} \left\{\left(\frac{\sigma!\rho! a_{\sigma,\rho}}{2^{(n+2\alpha)}}\right)\Phi\right\} \tag{18}$$

and Φ is given by (14). The phasor of the ω_q component of the output $y(t)$ is then given by

$$Y_q = \sum_{n=0}^{\infty} \sum_{\substack{\underbrace{n_1,\cdots,n_N} \\ |n_1|+\cdots+|n_N|=n}} U_q. \tag{19}$$

We have thus derived an algebraic formula for the output of a bivariate power series having two multifrequency inputs. These formulas reduce to those presented in [2] for a single variable power series with the elimination of the appropriate variables and subsequent grouping of terms.

III. Example: A Diode Ring Mixer

An example of a circuit that can be modeled using bivariate generalized power series analysis is the diode ring mixer shown in Fig. 1. In order to calculate a behavioral model for this entire circuit, we need to find an approximation to the output voltage V_{IF} as a function of the two input voltages V_{LO} and V_{RF}. Moreover, this approximation needs to be in the form of (3). Thus we will model the entire circuit as a two-input voltage-controlled voltage source.

The current–voltage relationship for the individual diodes is modeled by the Shockley diode equation:

$$I_j = I_{0j}(e^{V_j/V_t} - 1) \tag{20}$$

where I_j is the current through diode D_j, V_j is the voltage across D_j, $V_t = \eta kT/q$, I_{0j} is the saturation current for diode j, T is the junction temperature, k is Boltzmann's constant, and η is the ideality factor.

Assuming that the transformers are ideal, the KCL and KVL equations for this circuit reduce to

$$V_1(t) = \frac{1}{2}V_{\mathrm{LO}}(t) - \frac{1}{2}V_{\mathrm{RF}}(t) - V_{\mathrm{IF}}(t) \tag{21}$$

$$V_2(t) = \frac{1}{2}V_{\mathrm{LO}}(t) + \frac{1}{2}V_{\mathrm{RF}}(t) + V_{\mathrm{IF}}(t) \tag{22}$$

$$V_3(t) = \frac{1}{2}V_{\mathrm{RF}}(t) - \frac{1}{2}V_{\mathrm{LO}}(t) - V_{\mathrm{IF}}(t) \tag{23}$$

$$V_4(t) = V_{\mathrm{IF}}(t) - \frac{1}{2}V_{\mathrm{LO}}(t) - \frac{1}{2}V_{\mathrm{RF}}(t) \tag{24}$$

$$I_1(t) - I_2(t) + I_3(t) - I_4(t) - \frac{V_{\mathrm{IF}}(t)}{R_{\mathrm{IF}}} = 0. \tag{25}$$

The explicit notation of time (t) will be dropped for simplification.

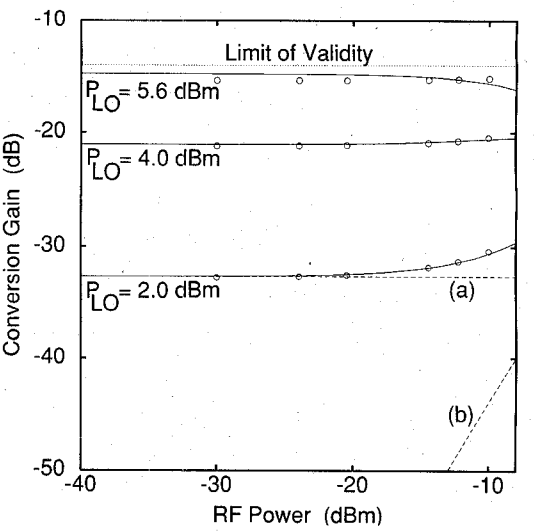

Fig. 2. Conversion gain for different LO power levels. Solid lines are bivariate GPSA calculations. Circles are ASTAP (time-domain simulation) calculations. Dashed lines are the first two terms of the decomposition of the solid line for $P_{\mathrm{LO}} = 2.0$ dBm. (a) is the constant term: RF^0. (b) is the second-order term: RF^2.

Equations (21)–(25) were solved for V_{IF} by means of the computer-algebra program MAPLE [7] to perform the algebra and calculus operations. Although all of the operations are straightforward, some of the equations are so large that manual calculations are impractical. As an intermediate step, a function f having the desired solution at $f = 0$ was obtained:

$$\begin{aligned} f = {} & I_{01}(e^{(1/2V_{\mathrm{LO}} - 1/2V_{\mathrm{RF}} - V_{\mathrm{IF}})/V_t} - 1) \\ & - I_{02}(e^{(1/2V_{\mathrm{LO}} + 1/2V_{\mathrm{RF}} + V_{\mathrm{IF}})/V_t} - 1) \\ & + I_{03}(e^{(1/2V_{\mathrm{RF}} - 1/2V_{\mathrm{LO}} - V_{\mathrm{IF}})/V_t} - 1) \\ & - I_{04}(e^{(V_{\mathrm{IF}} - 1/2V_{\mathrm{LO}} - 1/2V_{\mathrm{RF}})/V_t} - 1) - \frac{V_{\mathrm{IF}}}{R_{\mathrm{IF}}}. \end{aligned} \tag{26}$$

Since we want a closed-form solution for V_{IF}, we now estimate f by a third-degree Taylor series in V_{IF}:

$$\begin{aligned} f \approx {} & f(V_{\mathrm{IF}} = 0) + f'(V_{\mathrm{IF}} = 0)V_{\mathrm{IF}} + \frac{1}{2}f''(V_{\mathrm{IF}} = 0)V_{\mathrm{IF}}^2 \\ & + \frac{1}{6}f'''(V_{\mathrm{IF}} = 0)V_{\mathrm{IF}}^3. \end{aligned} \tag{27}$$

This third-order polynomial in V_{IF} can be solved in closed form [6]. In general, of the three solutions to this third-order equation, two are complex and one is real. Using the real solution, we get a very large equation which we will call g. The full solution of g is too large to be included here, but g has the form $V_{\mathrm{IF}} = g(V_{\mathrm{RF}}, V_{\mathrm{LO}}, I_{01}, I_{02}, I_{03}, I_{04}, V_t)$, to which a bivariate power series of the form

$$g(V_{\mathrm{RF}}, V_{\mathrm{LO}}) = \sum_{\sigma=0}^{9} \sum_{\rho=0}^{9} a_{\sigma,\rho} V_{\mathrm{RF}}^{\sigma} V_{\mathrm{LO}}^{\rho} \tag{28}$$

can be fitted using least-square techniques over a given range. Thus (28) has the form of (3) with $b_k = 1$, $\tau_{k,\sigma} = 0$, $d_k = 1$, and $\lambda_{k,\rho} = 0$. For our investigation we used the voltage ranges $-0.6 \leq V_{\mathrm{LO}} \leq 0.6$ and $-0.2 \leq V_{\mathrm{RF}} \leq 0.2$, and the rms fit error was less than 1%. For the ring mixer of Fig. 1, $\eta = 1$, $I_{01} = 1.00$ pA, $I_{02} = 1.01$ pA, $I_{03} = 1.03$ pA, $I_{04} = 1.06$ pA, $V_t = 0.02569$ V, and the transformers are ideal and have 1:1 turns ratios. The solid lines in Fig. 2 give the steady-state conversion power gain of

P_{IF}/P_{RF} for several LO powers. Since the power series (28) is valid only for a given range of the inputs, the macromodel is only valid within that range. The circles are simulation results using the time-domain simulator ASTAP [8], and show good agreement.

IV. Transfer Characteristics

The dashed lines in Fig. 2 demonstrate an important property of bivariate GPSA. Since the summation given by (19) contains powers of the phasor components as given by (14), any arbitrary input–ouptut transfer characteristic is of the form

$$Y_q = \sum_i H_{i,j}(X_j) \tag{29}$$

where $H_{i,j}$ is an ith-order nonlinear transfer function for the input phasor X_j (or set of X_j's). In general, $H_{i,j}$ is a function of the other input phasors. The dashed lines in Fig. 2 give (*a*) first-order, H_1, and (*b*) third-order, H_3, transfer characteristics for the IF phasor when $P_{LO} = 2.0$ dBm. In our example, the even-order transfer functions are zero. Note that in Fig. 2, the vertical axis is gain, not output amplitude; thus the lines represent the zeroth-order and second-order transfer characteristics for the gain, corresponding to the first- and third-order transfer characteristics for output amplitude. For the range modeled, all higher order transfer functions are negligible. Adding (*a*) and (*b*) yields a value within 1% of the total characteristic (solid line) shown for $P_{LO} = 2$ dBm. Thus a simple behavioral model is obtained by using only lower order powers of the input. Here, the nonlinear RF to IF characteristics can be described by the sum of two components. Each component can be represented as a linear function when expressed in log–log form.

V. Conclusion

The algebraic formula for the output of a nonlinearity described by a bivariate generalized power series having multifrequency inputs has been developed. These formulas enhance the capabilities of generalized power series analysis by allowing nonlinear functions of two variables to be considered in a general way. An example of a ring mixer has shown the practicality of this kind of analysis.

References

[1] S. L. Bussgang, L. Ehrman, and J. W. Graham, "Analysis of nonlinear systems with multiple inputs," *Proc. IEEE*, vol. 62, pp. 1088–1119, Aug. 1974.

[2] M. B. Steer and P. J. Khan, "An algebraic formula for the complex output of a system with multi-frequency excitation," *Proc. IEEE*, vol. 71, pp. 177–179, Jan. 1983.

[3] T. Narhi, "Multifrequency analysis of non-linear circuits using one and two dimensional series expansions," in *Proc. 19th European Microwave Conf.*, 1989.

[4] G. W. Rhyne, M. B. Steer, and B. D. Bates, "Frequency domain nonlinear circuit analysis using generalized power series," *IEEE Trans. Microwave Theory Tech.*, vol. 36, pp. 379–387, Feb. 1988.

[5] R. A. Nobakht, P. W. Pate, and S. H. Ardalan, "CAPSIM: A graphical simulation tool for communication systems," in *Proc. Globecom '88*, pp. 1692–1696.

[6] M. Abramowitz and I. A. Stegun, *Handbook of Mathematical Functions*. New York: Dover, 1965.

[7] B. W. Char, K. O. Geddes, G. H. Gonnet, and S. M. Watt, *Maple User's Guide*. Waterloo, Ont.: WATCOM Publications, 1985.

[8] W. T. Weeks *et al.*, "Algorithms for ASTAP—A network-analysis program," *IEEE Trans. Circuit Theory*, vol. CT-20, pp. 628–634, Nov. 1973.

Modeling of Asymmetric and Offset Gaps in Shielded Microstrips and Slotlines

ANIMESH BISWAS, MEMBER, IEEE, AND VIJAI K. TRIPATHI, SENIOR MEMBER, IEEE

***Abstract*—A generalized model for characterizing the frequency-dependent properties of general symmetric, asymmetric, and offset gaps in microstrips and slotlines on a single-layer or multilayer dielectric medium is presented. The transverse resonance technique is applied in the spectral domain to extract the equivalent circuit model parameters of the discontinuities. This technique incorporates the end effect of the discontinuity by a compatible choice of basis functions.**

I. Introduction

The characterization of symmetric and asymmetric gaps in microstrips and slotlines has been the subject of considerable interest in recent years since a knowledge of these discontinuity parameters is required for an accurate design of resonator elements and multiresonator filter circuits. The offset gaps in microstrips and slotlines provide an additional degree of freedom in terms of layout and design of coupled resonator filters. In addition, the analysis can also be helpful in estimating the coupling between offset coplanar conductors and slots in high-density microwave and millimeter-wave integrated circuits. A rigorous analysis for symmetric and asymmetric gaps in microstrips on suspended substrate has been presented by Koster and Jansen [1]. The accuracy of the method depends primarily on the choice of basis functions and can be verified by suitable experimental data. Experimental data for the end effect of open-ended slotline have been presented by Knorr [2]. This paper gives a general analysis of the gap discontinuities in both microstrip and slot structures, including offset gaps. The technique is based on an application of the transverse resonance technique proposed by Sorrentino and Itoh [3]. Here, the fields in various regions of the cavity are expanded in terms of hybrid modes whereas the slot fields and strip currents are expressed in terms of simple yet accurate basis functions. The validity of this type of basis function has been affirmed experimentally for the case of finline gap discontinuities [4].

II. Theory

The cross-sectional and longitudinal views of the general gap discontinuities in shielded microstrips and slotlines and their equivalent circuits are shown in Figs. 1 and 2. The electric and magnetic fields are expanded in terms of hybrid modes in each region and then the application of the boundary conditions at all the interfaces leads to the Green's dyadic as given in [4]. This is followed by the application of the Galerkin procedure in the transform domain, leading to a set of homogeneous equations as

Manuscript received October 10, 1989; revised December 15, 1989.

The authors are with the Department of Electrical and Computer Engineering, Oregon State University, Corvallis, OR 97331.

IEEE Log Number 9034894.